

Graph Neural Networks with Learnable and Optimal Polynomial Bases

Yuhe Guo¹ Zhewei Wei¹

Abstract

Polynomial filters, a kind of Graph Neural Networks, typically use a predetermined polynomial basis and learn the coefficients from the training data. It has been observed that the effectiveness of the model is highly dependent on the property of the polynomial basis. Consequently, two natural and fundamental questions arise: Can we learn a suitable polynomial basis from the training data? Can we determine the optimal polynomial basis for a given graph and node features?

In this paper, we propose two spectral GNN models that provide positive answers to the questions posed above. First, inspired by Favard’s Theorem, we propose the FavardGNN model, which learns a polynomial basis from the space of all possible orthonormal bases. Second, we examine the supposedly unsolvable definition of optimal polynomial basis from Wang & Zhang (2022) and propose a simple model, OptBasisGNN, which computes the optimal basis for a given graph structure and graph signal. Extensive experiments are conducted to demonstrate the effectiveness of our proposed models.

1. Introduction

Spectral Graph Neural Networks are a type of Graph Neural Networks that apply filtering operations on graph laplacian spectrums. To avoid eigen-decomposition, spectral GNNs approximate the desired filtering operations by polynomials of laplacian eigenvalues.

As categorized in He et al. (2022), there are mainly two kinds of spectral GNNs. In some works, the desired polynomial filters are **predefined**. For example, GCN (Kipf & Welling, 2017) fixes the filter to be $I - \hat{L}$, and APPNP (Klicpera et al., 2019) restricts the filtering function within the Personalized Pagerank.

¹Gaoling School of Artificial Intelligence, Renmin University of China. Correspondence to: Yuhe Guo <guoyuhe@ruc.edu.cn>, Zhewei Wei <zhewei@ruc.edu.cn>.

Another line of research approximates **arbitrary** filters with learnable polynomials. These models typically fix a predetermined polynomial basis and learn the coefficients from the training data. ChebNet (Defferrard et al., 2016) uses Chebyshev basis following the tradition of Graph Signal Processing (Hammond et al., 2009). GPRGNN (Chien et al., 2021) uses Monomial basis, which is straightforward. BernNet (He et al., 2021) uses the non-negative Bernstein basis for regularization and interpretation. JacobiConv (Wang & Zhang, 2022) chooses among the family of Jacobi polynomial bases, with the exact basis determined by two extra hyperparameters. ChebNetII (He et al., 2022) revisits the Chebyshev basis, and incorporates the power of Chebyshev interpolation by reparameterizing learnable coefficients by chebynodes. Please refer to Section 2.1 for more concrete backgrounds about polynomial filtering.

However, there are still two fundamental challenges on the choice of basis.

Challenge 1: It is well known that the choice of basis has a significant impact on practical performance. However, the proportion of known polynomial bases is small and may not include the best-fitting basis for a given graph and signal. Therefore, we pose the following question: **Can we learn a polynomial basis from the training data out of all possible orthonormal polynomials?**¹

Challenge 2: On the other hand, although these bases differ in empirical performances, their expressiveness should be the same: any target polynomial of order K can be represented by any complete polynomial basis with truncated order K (See Figure 1 for an example). Therefore, Wang & Zhang (2022) raised a definition of *optimal basis* from an optimization perspective, which promises an optimal convergence rate. However, this basis is believed to be unsolvable using existing techniques. Consequently, a natural question is: **can we compute this optimal basis for a given graph and signal using innovative techniques?**

In this paper, we provide positive answers to the questions posed above. We summarize our contributions in three folds. Firstly, we propose FavardGNN with **learnable orthonormal basis** to tackle the first challenge. The theoretical basis of FavardGNN is two Theorems in orthogonal polynomi-

¹For the concrete definition of orthonormal polynomial bases, please check the preliminaries in Section 2.2.

	$k=0$	$k=1$	$k=2$	Representation of $h(\lambda) = \lambda^2 + 1$
Monomial Basis	$M_0(\lambda) = 1$	$M_1(\lambda) = \lambda$	$M_2(\lambda) = \lambda^2$	$h(\lambda) = M_0 + M_2(\lambda)$
Chebyshev Basis	$T_0(\lambda) = 1$	$T_1(\lambda) = \lambda$	$T_2(\lambda) = \lambda^2 - 1$	$h(\lambda) = 2 \cdot T_0(\lambda) + T_2(\lambda)$
Bernstern Basis		$B_{k,2}(\lambda) = \binom{2}{k} \lambda^k (1-\lambda)^{2-k} \quad (k=0,1,2)$		$h(\lambda) = B_{0,2}(\lambda) + B_{1,2}(\lambda) + 2 \cdot B_{2,2}(\lambda)$
Jacobi Basis ($\alpha = \beta = 1$)	$P_0^{(\alpha, \beta)}(\lambda) = 1$	$P_1^{(\alpha, \beta)}(\lambda) = 2\lambda$	$P_2^{(\alpha, \beta)}(\lambda) = \frac{33}{8} + \frac{15}{4}\lambda + \frac{15}{8}\lambda^2$	$h(\lambda) = -\frac{18}{15}P_0^{(\alpha, \beta)} - P_1^{(\alpha, \beta)} + \frac{8}{15}P_2^{(\alpha, \beta)}$

Figure 1. Representation of $h(\lambda) = \lambda^2 + 1$ by different bases.

als: the Three-term recurrences and its converse, Favard’s Theorem. FavardGNN learns from the *whole space* of possible orthonormal basis with $2(K+1)$ extra parameters². Secondly, we propose OptBasisGNN with **solvable optimal basis**. We solve the optimal basis raised by Wang & Zhang (2022) by avoiding the explicit solving of the weight function. Note that, although we write out the implicitly defined/solved polynomial series in the methodology section, we never need to solve it explicitly. Last but not least, we conduct **extensive experiments** to demonstrate the effectiveness of our proposed models.

2. Background and Preliminaries

2.1. Background of Spectral GNNs

In this section, we provide some necessary backgrounds of spectral graph neural networks, and show how the choice of polynomial bases emerges as a problem. Notations used are summarized in Table 6 in Appendix A.

Graph Fourier Transform. Consider an undirected and connected graph $G = (V, E)$ with N nodes, its symmetric normalized adjacency matrix and laplacian matrix are denoted as \hat{P} and \hat{L} , respectively, $\hat{L} = I - \hat{P}$. *Graph Fourier Transform*, as defined in the spatial/spectral domain of graph signal processing, is analogous to the time/frequency domain Fourier Transform (Hammond et al., 2009; Shuman et al., 2013). One column in the representations of N nodes, $X \in \mathbb{R}^{N \times d}$, is considered a *graph signal*, denoted as x . The complete set of N eigenvectors of \hat{L} , denoted as U , who show varying structural frequency characteristics (Shuman et al., 2013), are used as *frequency components*. *Graph Fourier Transform* is defined as $\hat{x} := U^T x$, where signal x is projected to the frequency responses of all components. It is then followed by *modulation*, which suppresses or strengthens certain frequency components, denoted as $\hat{x}^* := \text{diag}\{\theta_0, \dots, \theta_{N-1}\}\hat{x}$. After modulation, *inverse Fourier Transform*: $x^* := U\hat{x}^*$ transforms \hat{x}^* back to the spatial domain. The three operations form the process of *spectral filtering*: $U \text{diag}\{\theta_0, \theta_1, \dots, \theta_{N-1}\}U^T x$ (1).

Polynomial Approximated Filtering. In order to avoid time-consuming eigen-decomposition, a line of work ap-

proximate θ_i by polynomial function of λ_i , which is the i -th eigenvalue of \hat{L} , i.e. $\theta_i \approx h(\lambda_i)$. Equation (1) then becomes a form that is easy for fast *localized* calculation: $U \text{diag}\{h(\lambda_0), h(\lambda_1), \dots, h(\lambda_{N-1})\}U^T x = h(\hat{L})x$.

As listed in Introduction, various *polynomial bases* have been utilized, denoted as $h(\lambda) = \sum_{k=0}^K \alpha_k g_k(\lambda)$. The filtering process on the input signal x is then expressed as $x \rightarrow z = \sum_{k=0}^K \alpha_k g_k(\hat{P})x$. When considering independent filtering on each channel of the node feature matrix X simultaneously, the **multichannel filtering** can be denoted as: $X \rightarrow Z = \sum_{l \in [1, h]} \sum_{k=0}^K \alpha_{k,l} g_{k,l}(\hat{P})X_{:,l}$ (2).

For further simplicity, we equivalently use $b(\hat{P})$ instead of $h(\hat{L})$ in this paper, where $b(\hat{P}) := h(I - \hat{P})$. Note that $b(\cdot)$ is defined on the spectrum of \hat{P} , and the i -th eigenvalue of \hat{P} , denoted as μ_i , equals $1 - \lambda_i$.

2.2. Orthogonal and Orthonormal Polynomials

In this section, we give a formal definition of orthogonal and orthonormal polynomials, which plays a central role in the choosing of polynomial bases (Simon, 2014).

Inner Products. The inner product of polynomials is defined as $\langle f, g \rangle := \int_a^b f(x)g(x)w(x)dx$, where f, g and w are functions of x on interval (a, b) , and the *weight function* w should be non-negative to guarantee the positive-definiteness of inner-product space.

The definition of the inner products induces the definitions of *norm* and *orthogonality*. The norm of polynomial f is defined as: $\|f\| = \sqrt{\langle f, f \rangle}$, and f and g are orthogonal to each other when $\langle f, g \rangle = 0$. Notice that the concept of inner product, norm, and orthogonality are all defined with respect to some weight function.

Orthogonal Polynomials. A sequence of polynomials $\{p_n(x)\}_{n=0}^{\infty}$ where $p_n(x)$ is of exact degree n , is called *orthogonal* w.r.t. the positive weight function $w(x)$ if, for $m, n = 0, 1, 2, \dots$, there exists $\langle p_n, p_m \rangle = \delta_{mn} \|p_n\|^2$ ($\|p_n\|^2 \neq 0$), where the inner product $\langle f, g \rangle$ is defined w.r.t. $w(x)$. When $\|p_n\|^2 = 1$ for $n = 0, 1, 2, \dots$, $\{p_n(x)\}_{n=0}^{\infty}$ is known as **orthonormal** polynomial series.

When a weight function is given, the orthogonal or orthonor-

² K is the truncated order of polynomial series.

Algorithm 1: FAVARDFILTERING

Input: Input signals X with d channels; Normalized graph \hat{P} ; Truncated polynomial order K

Learnable Parameters: β, γ, α

Output: Filtered Signals Z

```

1  $x_{-1} \leftarrow 0$ 
2 for  $l = 0$  to  $d - 1$  do
3    $x \leftarrow X_{:,l}$ ,  $x_0 \leftarrow x / \sqrt{\beta_{0,l}}$ ,  $z \leftarrow \alpha_{0,l} x_0$ 
4   for  $k = 0$  to  $K$  do
5      $x_{k+1} \leftarrow$ 
        $(\hat{P}x_k - \gamma_{k,l}x_k - \sqrt{\beta_{k,l}}x_{k-1}) / \sqrt{\beta_{k+1,l}}$ 
6      $z \leftarrow z + \alpha_{k+1,l}x_{k+1}$ 
7    $Z_{:,l} \leftarrow z$ 
8 return  $Z$ 

```

mal series with respect to the weight function can be solved by *Gram-Schmidt process*.

Remark 2.1. In this paper, the orthogonal/orthonormal polynomial bases we consider are truncated polynomial series, i.e. the polynomials that form a basis are of increasing order.

3. Learnable Basis via Favard's Theorem

Empirically, spectral GNNs with different polynomial bases vary in performance on different datasets, which leads to two observations: (1) the choice of bases matters; (2) whether a basis is preferred might be related to the input, i.e. different signals on their accompanying underlying graphs.

For the first observation, we notice that up to now, polynomial filters *pick* polynomial bases from well-studied polynomials, e.g. Chebyshev polynomials, Bernstein polynomials, *etc*, which narrows down the range of choice. For the second observation, we question the reasonableness of fixing a basis during training. A related effort is made by Jacobi-Conv (Wang et al., 2019), who adapt to a Jacobi polynomial series from the family of Jacobi polynomials via *hyperparameter tuning*. However, the range they choose from is discrete. Therefore, we aim at dynamically **learn** polynomial basis from the input from a **vast range**.

3.1. Recurrence Formula for Orthonormal Bases

Luckily, the Three-term recurrences and Favard's theorem of orthonormal polynomials provide a *continuous* parameter space to learn basis. Generally speaking, three-term recurrences states that every orthonormal polynomial series satisfies a very characteristic form of recurrence relation, and Favard's theorem states the converse.

Theorem 3.1 (Three Term Recurrences for Orthonormal Polynomials). (Gautschi, 2004, p. 12) *For orthonormal polynomials $\{p_k\}_{k=0}^{\infty}$ w.r.t. weight function w , suppose that the leading coefficients of all polynomials are positive, there*

Algorithm 2: FAVARDGNN (For Classification)

Input: Raw features X_{raw} ; Normalized graph \hat{P} ; Truncated polynomial order K

Learnable Parameters: $W_0, b_0, W_1, b_1, \beta, \gamma, \alpha$

Output: Label predictions \hat{Y}

```

1    $X \leftarrow X_{raw}W_0 + b_0$ 
2    $Z \leftarrow \text{FAVARDFILTERING}(X, \hat{P}, K, \beta, \gamma, \alpha)$ 
3    $\hat{Y} \leftarrow \text{Softmax}(ZW_1 + b_1)$ 

```

exists the three-term recurrence relation:

$$\begin{aligned} \sqrt{\beta_{k+1}} p_{k+1}(x) &= (x - \gamma_k) p_k(x) - \sqrt{\beta_k} p_{k-1}(x), \\ p_{-1}(x) &:= 0, \quad p_0(x) = 1 / \sqrt{\beta_0}, \\ \gamma_k &\in \mathbb{R}, \quad \sqrt{\beta_k} \in \mathbb{R}^+, \quad k \geq 0 \end{aligned} \quad (3)$$

with $\beta_0 = \int w(x)dx$.

Theorem 3.2 (Favard's Theorem; Orthonormal Case). (Favard, 1935), (Simon, 2005, p. 14) *A polynomial series $\{p_k\}_{k=0}^{\infty}$ who satisfies the recurrence relation in Equation (3) is orthonormal w.r.t. a weight function w that $\beta_0 = \int w(x)dx$.*

By Theorem 3.2, any possible recurrences with the form (3) defines an orthonormal basis. By Theorem 3.1, such a formula covers the whole space of orthonormal polynomials. If we set $\{\sqrt{\beta_k}\}$ and $\{\gamma_k\}$ to be learnable parameters with $\sqrt{\beta_k} > 0 (k \geq 0)$, any orthonormal basis can be obtained.

We put the more general *orthogonal* form of Theorem 3.1 and Theorem 3.2 in Appendix B.1 to B.5. In fact, the property of three-term recurrences for orthogonal polynomials has been used multiple times in the context of current spectral GNNs to reuse $g_k(\hat{P})x$ and $g_{k-1}(\hat{P})x$ for the calculation of $g_{k+1}(\hat{P})x$. Defferrard et al. (2016) owe the fast filtering of ChebNet to employing the three-term recurrences of *Chebyshev polynomials* (the first kind, which is orthogonal w.r.t. $\frac{1}{\sqrt{x^2-1}}$): $T_{k+1}(x) = 2xT_k(x) - T_{k-1}(x)$. Similarly, JacobiConv (Wang & Zhang, 2022) employs the three-term recurrences for *Jacobi polynomials* (orthogonal w.r.t. to $(1-x)^a(1+x)^b$). In this paper, however, we focus on orthonormal bases because they minimize the mutual influence of basis polynomials and the influence of the unequal norms of different basis polynomials.

3.2. FavardGNN

Formulation of FavardGNN. We formally write the architecture of FAVARDGNN (Algorithm 2), with the filtering process illustrated in FAVARDFILTERING (Algorithm 1). Note that the iterative process of Algorithm 1 (lines 3-5) follows exactly from Equation (3) in Favard's Theorem. The key insight is to treat the coefficients β, γ, α in Equation (3) as learnable parameters. Since Theorem 3.1 and

Theorem 3.2 state that the orthonormal basis must satisfy the employed iteration and vice versa, it follows that the model can learn a suitable orthonormal polynomial basis from among all possible orthonormal bases.

Following convention, before FAVARDFILTERING, an MLP is used to map the raw features onto the signal channels (often much less than the dimension of raw features). In regression problems, the filtered signals are directly used as predictions; for classification problems, they are combined by another MLP followed by a softmax layer.

Parallel Execution. Note that for convenience of presentation, we write the FAVARDFILTERING Algorithm in a form of nested loops. In fact, the computation on different channels (the inner loop k) is conducted simultaneously. We put more concrete implementation in PyTorch-styled the pseudocode in Appendix C.1.

3.3. Weaknesses of FavardGNN

However, there are still two main weaknesses of FavardGNN. Firstly, the orthogonality lacks interpretability. The weight function w can only be solved analytically in a number of cases (Geronimo & Van Assche, 1991). Even if the weight function is solved, the form of w might be too complicated to understand.

Secondly, FAVARDFILTERING is not good in convergence properties: consider a simplified optimization problem $\min \|Z - Y\|_F^2$ which has been examined in the context of GNN (Xu et al., 2021; Wang & Zhang, 2022), even this problem is non-convex w.r.t the learnable parameters in Z . We will re-examine this problem in the experiment section.

4. Achieving Optimal Basis

Although FavardGNN has the potential to reach the whole space of orthonormal polynomial series, on the other hand, we still want to know: **whether there is an optimal and accessible basis** in this vast space.

Recently, Wang & Zhang (2022) raises a criterion for optimal basis. Since different bases are the same in expressiveness, this criterion is induced from an angle of optimization. However, Wang & Zhang (2022) believe that this optimal basis is unreachable. In this section, we follow this definition of optimal basis, and show how we can use exactly this optimal basis with $O(K|E|)$ time complexity.

4.1. A Criterion for Optimal Basis

We will firstly restate the related section of Wang & Zhang (2022) very briefly, with a more complete review put in Appendix E.

Definition of Optimal Basis. Wang & Zhang (2022)

Algorithm 3: (An Unreachable Algorithm for Getting Optimal Basis)

Input: Graph signal x ; Normalized graph adjacency \hat{P} ; Truncated polynomial order K .

Output: Optimal basis $\{g_k(\cdot)\}_{k=0}^K$

- 1 $U, \{\mu_i\}_{i=1}^N \leftarrow$ Eigen decomposition of \hat{P}
- 2 Calculate $f(\mu)$ as described in E.1
- 3 Use Gram-Schmidt process and weight function $f(\mu)$ to construct an orthonormal basis $\{g_k\}_{k=0}^K$

considers the squared loss $R = \frac{1}{2}\|Z - Y\|_F^2$, where Y is the target signal. Since each signal channel contributes independently to the loss, the authors then consider the loss function channelwisely and ignore the index l , that is, $r = \frac{1}{2}\|z - y\|_F^2$, where $z = \sum_{k=0}^K \alpha_k g_k(\hat{P})x$.

Since r is convex w.r.t. α , the gradient descents' convergence rate reaches optimal when the **Hessian matrix** is an identity matrix. The (k_1, k_2) element of Hessian matrix is:

$$H_{k_1 k_2} = \frac{\partial r}{\partial \alpha_{k_1} \alpha_{k_2}} = x^T g_{k_2}(\hat{P}) g_{k_1}(\hat{P}) x. \quad (4)$$

Definition 4.1 (Optimal basis for signal x). For a given graph signal x , polynomial basis $\{g_k\}_{k=0}^K$ is optimal in convergence rate when H given in (4) is an **identity matrix**.

Unachievable Algorithm Towards Optimal Basis.

Wang & Zhang (2022) continue to rewrite Equation (4) by Riemann sum: $H_{k_1 k_2} = \int_{\mu=-1}^1 g_{k_1}(\mu) g_{k_2}(\mu) f(\mu) d\mu$, where $f(\mu)$ is given below (Remark 4.2), and Definition 4.1 is reached when $\{g_k(\cdot)\}_{k=0}^K$ is orthonormal polynomial basis w.r.t. $f(\cdot)$.

Remark 4.2. The **exact form of the weight function** of optimal basis defined in Definition 4.1 is $f(\mu) = \frac{\Delta F(\mu)}{\Delta \mu}$, where $F(\mu) := \sum_{\mu_i \leq \mu} (U^T x)_i^2$.

Having write out the weight function $f(\mu)$, the optimal basis is determined. Wang & Zhang (2022) think of a regular process for getting this optimal basis, which is unreachable since eigen-decomposition is unaffordable for large graphs. We summarize this process in Algorithm 3.

As a result, Wang & Zhang (2022) come up with a compromised method that allows the model to choose from the family of orthogonal Jacobi bases, who have "flexible enough weight functions", i.e. $(1 - \mu)^a (1 + \mu)^b$, determined by two hyper-parameters a and b . However, still, a very small fraction of possible weight functions are covered, possibly without the optimal weight function in Remark 4.2.

Algorithm 4: OBTAINNEXTBASISVECTOR (RAW VERSION)

Input: Normalized graph \hat{P} ; Solved basis vectors v_0, \dots, v_k ($k \geq 0$)

Output: v_{k+1}

- 1 Step 1: $v_{k+1}^* \leftarrow \hat{P}v_k$
- 2 Step 2: $v_{k+1}^\perp \leftarrow v_{k+1}^* - \sum_{i=0}^k \langle v_{k+1}^*, v_i \rangle v_i$
- 3 Step 3: $v_{k+1} \leftarrow v_{k+1}^\perp / \|v_{k+1}^\perp\|$
- 4 **return** v_{k+1}

4.2. From Polynomial Basis to Vector Basis

In this section, we show that the optimal bases given in Definition 4.1 can be solved efficiently in $O(K|E|)$. Instead of following the three-step convention of Algorithm 3, we use the optimal bases **without** explicitly solving the $f(\mu)$ and $\{g_k(\mu)\}_{k=0}^K$ as pre-steps of polynomial filtering.

The key insight of our method is to consider the inner product space of vectors rather than that of polynomials. We shift our attention from solving orthonormal polynomial basis $g_k(x)$ (w.r.t. a specific weight function) to orthonormal vector basis $g_k(\hat{P})x$. Thus, we avoid the need to solve for the *inaccessible weight function* in the habitual procedure 3, making the optimal polynomial series attainable.

Optimal Vector Basis. Following Wang & Zhang (2022), we consider $x \rightarrow z = \sum_{k=0}^K \alpha_k g_k(\hat{P})x$ on one channel. Instead of taking $\sum_{k=0}^K \alpha_k g_k(\hat{P}) = b(\hat{P})$ as a whole, we now regard $\{v_k | v_k := g_k(\hat{P})x\}_{k=0}^K$ as a *vector basis*. Thus, the filtered signal z is a linear combination of $\{v_k\}_{k=0}^K$.

By Definition 4.1, the optimal basis is achieved when

$$v_{k_2}^T v_{k_1} = x^T g_{k_2}(\hat{P}) g_{k_1}(\hat{P}) x = \delta_{k_1 k_2},$$

which is equivalent to finding a vector basis $\{v_k\}_{k=0}^K$ that satisfies two conditions: **Condition 1:** Orthonormality.

Condition 2: Polynomials with **increasing order**, that is, for $k = 0, 1, \dots, K$, there exists a polynomial g_k so that $v_k = g_k(\hat{P})x$, where $g_k(\cdot)$ is of order k .

Algorithm 4 raw illustrates the pseudocode for obtaining the vector basis that satisfies the aforementioned two conditions. We can get v_{k+1} by firstly calculate $v_{k+1}^* = \hat{P}v_k$, and then obtain v_{k+1} from v_{k+1}^* . The first step implicitly *raises the order* of $g_k(\cdot)$ by setting $v_{k+1}^* = \hat{P}v_k = \hat{P}g_k(\hat{P})x$. Then we calculate v_{k+1}^\perp which is orthogonal to previous basis vectors, and normalize it to obtain v_{k+1} . It is easy to see that v_0, \dots, v_{k+1} satisfies the two conditions required for optimal basis.

Achieving Linear Time Complexity. However, when conducting Algorithm 4 recursively until v_K is obtained,

Algorithm 5: OBTAINNEXTBASISVECTOR

(In comment, we write the the $(k+1)$ -th optimal basis polynomial $g_{k+1}(\cdot)$ based on $g_k(\cdot)$ and $g_{-1}(\cdot)$ that is implicitly used, but never solved explicitly.)

Input: Normalized graph \hat{P} ; Two solved basis vectors v_{k-1}, v_k ($k \geq 0$)

Output: v_{k+1}

- 1 Step 1: $v_{k+1}^* \leftarrow \hat{P}v_k$ // $g_{k+1}^*(\mu) := \mu g_k(\mu)$
- 2 Step 2:
$$v_{k+1}^\perp \leftarrow v_{k+1}^* - \langle v_{k+1}^*, v_k \rangle v_k - \langle v_{k+1}^*, v_{k-1} \rangle v_{k-1}$$
// $g_{k+1}^*(\mu) := g_{k+1}^*(\mu) - \langle v_{k+1}^*, v_k \rangle g_k(\mu) - \langle v_{k+1}^*, v_{k-1} \rangle g_{k-1}(\mu)$
- 3 Step 3: $v_{k+1} \leftarrow v_{k+1}^\perp / \|v_{k+1}^\perp\|$ // $g_{k+1}(\mu) := g_{k+1}^*(\mu) / \|v_{k+1}^\perp\|$
- 4 **return** v_{k+1}

Step 2 in total costs $O(K^2|E|)$. This would be inferior to ChebNet and GPRGNN, whose costs are $O(K|E|)$. Luckily, in Proposition 6, we show that in Step 2, instead of subtracting all the former vectors, we just need to subtract v_k and v_{k-1} from v_{k+1}^* .

Proposition 4.3. In Algorithm 4, v_{k+1}^* is only dependent with v_k and v_{k-1} .

Proof. Firstly, from the construction of v_{i+1} (Algorithm 4, $k = i$), we know that v_{i+1} is composed of $\{v_j\}_{j=0}^{j=i}$ and $\hat{P}v_i$. Therefore, $\hat{P}v_i$ can be expressed as weighted sum of $\{v_j\}_{j=0}^{j=i+1}$: $\hat{P}v_i = t_{i+1}v_{i+1} + t_i v_i + \dots + t_0 v_0$. Secondly, notice that $\langle \hat{P}v_k, v_i \rangle = v_k^T \hat{P}v_i = \langle v_k, \hat{P}v_i \rangle$. We get

$$\langle v_k, \hat{P}v_i \rangle = \left\langle v_k, \sum_{j=0}^{j=i+1} t_j v_j \right\rangle = \sum_{j=0}^{j=i+1} t_j \langle v_k, v_j \rangle,$$

which equals 0 when $i \leq k-2$. \square

Remark 4.4. The insight is hugely inspired by the core proof part of the Theorem B.1 (Appendix B.1, the Three Term Recurrences for Orthogonal Polynomials), which shows that $x p_k(x)$ is only relevant to $p_{k+1}(x)$, $p_k(x)$ and $p_{k-1}(x)$. The difference is the shifting of consideration of inner production from the polynomial space to the vector space.

From Proposition 4.3, we get an improved algorithm (Algorithm 5) to obtain the *next* basis. By applying Algorithm 5 recursively, we get the optimal basis in Definition 1 efficiently.

Implicitly Solved Polynomial Basis. Looking back on Remark 4.2 and Algorithm 3, note that, though we don't *explicitly solve* the weight function and polynomials, we in fact *implicitly define* an orthonormal polynomial basis by three-term recurrence relations. We illustrate such recur-

rence in the comment of Algorithm 5, which can be written as:

$$\begin{aligned} \|v_{k+1}^\perp\| g_{k+1}(\mu) &= \mu g_k(\mu) - \langle v_{k+1}^*, v_k \rangle g_k(\mu) \\ &- \langle v_{k+1}^*, v_{k-1} \rangle g_{v_{k-1}}(\mu). \end{aligned} \quad (5)$$

Now, we confirm that, Equation (5) is consistent with the recurrence formula given in Equation (3). We show $\|v_k^\perp\| = \langle v_{k+1}^*, v_{k-1} \rangle$ (6) in Appendix B.6.

4.3. Formulation of OptBasisGNN

We show the procedure of OPTBASISFILTERING in Algorithm 6, which is the core part of the complete OptBasisGNN. Other parts of OptBasisGNN are MLP layers and softmax layers, same as in FAVARDGNN (Algorithm 2). The process of calculating the next basis vector and filtering on all channels are conducted in parallel. Please check the Pytorch-style pseudo-code in Appendix C.2.

Relation to FavardGNN. OptBasisGNN is a **particular case** of FavardGNN. FavardGNN is possible to reach the whole space of orthonormal bases, among all these bases, while OptBasis is the one that promises optimal convergence property.

Algorithm 6: OPTBASISFILTERING

Input: Input signals X with d channels; Normalized Graph \hat{P} ; Order K
Learnable Parameters : α
Output: Filtered signals Z

```

1  $v_{-1} \leftarrow 0$ 
2 for  $l = 0$  to  $d - 1$  do
3    $x \leftarrow X_{:,l}$ ,  $v_0 \leftarrow x / \|x\|$ ,  $z \leftarrow \alpha_{0,l} v_0$ 
4   for  $k = 0$  to  $K$  do
5      $v_{k+1} \leftarrow \text{OBTAINNEXTBASISVECTOR}(\hat{P}, v_k,$ 
        $v_{k-1})$ 
6      $z \leftarrow z + \alpha_{k+1,l} v_{k+1}$ 
7    $Z_{:,l} \leftarrow z$ 
8 return  $Z$ 

```

4.4. Scale Up OptBasisGNN

Scaling up GNNs on large graphs is a challenging and important problem. One way to scale up GNN models is to decouple feature propagation and transformation (Chen et al., 2020a; Wu et al., 2019; He et al., 2022). Similarly, we scale up OptBasisGNN by (1) drop the MLP layer before OPTBASISFILTERING, thus, the basis vectors for each channel are fixed; (2) **preprocess** the whole set of basis vectors (denote as $V \in R^{d \times (K+1) \times N}$) on CPU, and (3) conduct **batch training**: for each batch of nodes \mathcal{B} , move the corresponding segment of basis vectors $V[:, :, \mathcal{B}]$ to GPU.

5. Experiments

In this section, we conduct a series of comprehensive experiments to demonstrate the effectiveness of the proposed methods. Experiments consist of node classification tasks on small and large graphs, the learning of multi-channel filters, and a comparison of FavardGNN and OptBasisGNN.

5.1. Node Classification

Experimental Setup. We include medium-sized graph datasets conventionally used in preceding graph filtering works, including three heterophilic datasets (Chameleon, Squirrel, Actor) provided by Pei et al. (2020) and two citation datasets (PubMed, Citeseer) provided by Yang et al. (2016) and Sen et al. (2008). For all these graphs, we take a 60%/20%/20% train/validation/test split proportion following former works, e.g. Chien et al. (2021). We report our results of twenty runs over random splits with random initialization seeds. For baselines, we choose sota spectral GNNs. For other experimental settings, please refer to Appendix D.1. Besides, for evaluation of OptBasisGNN, please also check the results in the scalability experimental section (Section 5.2).

Results. As shown in Table 1, FavardGNN and OptBasisGNN outperform most strong baselines. Especially, in Chameleon, Squirrel and Actor, we see a big lift. The vast selection range and learnable nature of FavardGNN and the optimality of convergence provided by OptBasisGNN both enhance the performance of polynomial filters, and their performances hold flat.

5.2. Node Classification on Large Datasets

Experimental Setup. We perform node classification tasks on two large citation networks: ogbn-arxiv and ogbn-papers100M (Hu et al., 2020), and five large non-homophilic networks from the LINKX datasets (Lim et al., 2021). Except for Penn94, Genius and Twitch-Gamers, all other mentioned datasets use the scaled version of OptBasisGNN.

For ogbn datasets, we run repeating experiments on the given split with ten random model seeds, and choose baselines following the scalability experiments in ChebNetII (He et al., 2022). For LINKX datasets, we use the five given splits to align with other reported experiment results for Penn94, Genius, Twitch-Gamer and Pokec. For Wiki dataset, since the splits are not provided, we use five random splits. For baselines, we choose spectral GNNs as well as top-performing spatial models reported in Lim et al. (2021), including LINK, LINKX, GCNII (Chen et al., 2020b) and MixHop (Abu-El-Haija et al., 2019). For more detailed experimental settings, please refer to Appendix D.1.

Results. As shown in Table 2 and Table 3, On Penn94, Genius and Twitch-gamer, our two models achieve compa-

Table 1. Experimental results. *Accuracies \pm 95% confidence intervals* are displayed for each model on each dataset. The best-performing two results are highlighted. The results of GPRGNN are taken from He et al. (2021). The results of BernNet, ChebNetII and JacobiConv are taken from original papers. The results of FavardGNN and OptBasisGNN are the average of repeating experiments over 20 cross-validation splits.

Dataset	Chameleon	Squirrel	Actor	Citeseer	Pubmed
$\ V\ $	2,277	5,201	7,600	3,327	19,717
$\mathcal{H}(G)$.23	.22	.22	.74	.80
MLP	46.59 \pm 1.84	31.01 \pm 1.18	40.18 \pm 0.55	76.52 \pm 0.89	86.14 \pm 0.25
GCN	60.81 \pm 2.95	45.87 \pm 0.8	33.26 \pm 1.15	79.85 \pm 0.78	86.79 \pm 0.31
ChebNet	59.51 \pm 1.25	40.81 \pm 0.42	37.42 \pm 0.58	79.33 \pm 0.57	87.82 \pm 0.24
ARMA	60.21 \pm 1.00	36.27 \pm 0.62	37.67 \pm 0.54	80.04 \pm 0.55	86.93 \pm 0.24
APPNP	52.15 \pm 1.79	35.71 \pm 0.78	39.76 \pm 0.49	80.47 \pm 0.73	88.13 \pm 0.33
GPRGNN	67.49 \pm 1.38	50.43 \pm 1.89	39.91 \pm 0.62	80.13 \pm 0.84	88.46 \pm 0.31
BernNet	68.53 \pm 1.68	51.39 \pm 0.92	41.71 \pm 1.12	80.08 \pm 0.75	88.51 \pm 0.39
ChebNetII	71.37 \pm 1.01	57.72 \pm 0.59	41.75 \pm 1.07	80.53 \pm 0.79	88.93 \pm 0.29
JacobiConv	74.20 \pm 1.03	57.38 \pm 1.25	41.17 \pm 0.64	80.78 \pm 0.79	89.62 \pm 0.41
FavardGNN	72.32 \pm 1.90	63.49 \pm 1.47	43.05 \pm 0.53	81.89 \pm 0.63	90.90 \pm 0.27
OptBasisGNN	74.26 \pm 0.74	63.62 \pm 0.76	42.39 \pm 0.52	80.58 \pm 0.82	90.30 \pm 0.19

Table 2. Experimental results of large-scale datasets (non-homophilous). *Accuracies \pm standard errors* are displayed for each model on each dataset. The best-performing two results are highlighted. Results of BernNet and ChebNet are taken from He et al. (2022). Other results are from Lim et al. (2021). **Note** that for the large Pokec and Wiki datasets, we use the *scaled-up* version of OptBasisGNN, which is introduced in Section 4.4.

Dataset	Penn94	Genius	Twitch-Gamers	Pokec	Wiki
$\ V\ $	41,554	421,961	168,114	1,632,803	1,925,342
$\ E\ $	1,362,229	984,979	6,797,557	30,622,564	303,434,860
$\mathcal{H}(G)$.470	.618	.545	.445	.389
MLP	73.61 \pm 0.40	86.68 \pm 0.09	60.92 \pm 0.07	62.37 \pm 0.02	37.38 \pm 0.21
GCN	82.47 \pm 0.27	87.42 \pm 0.31	62.18 \pm 0.26	75.45 \pm 0.17	OOM
GCNII	82.92 \pm 0.59	90.24 \pm 0.09	63.39 \pm 0.61	78.94 \pm 0.11	OOM
MixHop	83.47 \pm 0.71	90.58 \pm 0.16	65.64 \pm 0.27	81.07 \pm 0.16	49.15 \pm 0.26
LINK	80.79 \pm 0.49	73.56 \pm 0.14	64.85 \pm 0.21	80.54 \pm 0.03	57.11 \pm 0.26
LINKX	84.71 \pm 0.52	90.77 \pm 0.27	66.06 \pm 0.19	82.04 \pm 0.07	59.80 \pm 0.41
GPRGNN	83.54 \pm 0.32	90.15 \pm 0.30	62.59 \pm 0.38	80.74 \pm 0.22	58.73 \pm 0.34
BernNet	83.26 \pm 0.29	90.47 \pm 0.33	64.27 \pm 0.31	81.67 \pm 0.17	59.02 \pm 0.29
ChebNetII	84.86 \pm 0.33	90.85 \pm 0.32	65.03 \pm 0.27	82.33 \pm 0.28	60.95 \pm 0.39
FavardGNN	84.92 \pm 0.41	90.29 \pm 0.14	64.26 \pm 0.12	-	-
OptBasisGNN	84.85 \pm 0.39	90.83 \pm 0.11	65.17 \pm 0.16	82.83 \pm 0.04	61.85 \pm 0.03

Table 3. Experimental results of large-scale datasets (ogbn-citation datasets). *Accuracies \pm 95% standard errors* are displayed. Besides OptBasisGNN, all the reported results are taken from ChebNetII. The dash line in BernNet means failing in preprocessing basis vectors in 24 hrs. Fixed splits of train/validation/test sets are used. 10 random model seeds are used for repeating experiments.

Dataset	ogbn-arxiv	ogbn-papers100M
$\ V\ $	169,343	111,059,956
$\ E\ $	1,166,243	1,615,685,872
$\mathcal{H}(G)$	0.66	-
GCN	71.74 \pm 0.29	OOM
ChebNet	71.12 \pm 0.22	OOM
ARMA	71.47 \pm 0.25	OOM
GPRGNN	71.78 \pm 0.18	65.89 \pm 0.35
BernNet	71.96 \pm 0.27	-
SIGN	71.95 \pm 0.12	65.68 \pm 0.16
GBP	71.21 \pm 0.17	65.23 \pm 0.31
NDLS*	72.24 \pm 0.21	65.61 \pm 0.29
ChebNetII	72.32 \pm 0.23	67.18 \pm 0.32
OptBasisGNN	72.27 \pm 0.15	67.22 \pm 0.15

table results to those of the sota spectral methods. On ogbn datasets as well as Pokec and Wiki with tens or hundreds of edges, we use the scaled version of OptBasisGNN with batch training. We do not conduct FavardGNN on these datasets, since the basis vectors of FavardGNN are cannot be precomputed. Notably, on Wiki dataset, the largest non-homophilous dataset, our method surpasses the second

top method by nearly one percent, this demonstrates the effectiveness of our scaled-up version of OptBasisGNN.

5.3. Learning Multi-Channel Filters from Signals

Experimental Setup. We extend the experiment of learning filters in He et al. (2021) and Balcilar et al. (2021). The differences are twofold: First, we consider the case of *multi-channel* input signals and learn filters *channelwisely*. Second, the *only* learnable parameters are the coefficients α . Note that the optimization target of this experiment is identical to how the optimal basis was derived by Wang & Zhang (2022) (See Section 4.1).

Table 4. Illustration of our multichannel filter learning experiment.

Original Image	Y: Band Reject	Y: Low Pass
Cl: Low pass		
Cb: Band Reject		
Cr: High Pass		

We put the practical background of our multichannel ex-

periment in YCbCr color space. Each 100×100 image is considered as a grid graph with input node signals on three channels: Y, Cb and Cr. Each signal might be filtered by complex filtering operations defined in (He et al., 2021). As shown in Table 4, using different filters on each channel results in different combination effects. We create a synthetic dataset with 60 samples from 15 original images. More about the synthetic dataset are in Appendix D.2.

Following He et al. (2021), we use input signals X and the true filtered signals Y to supervise the learning process of α . The optimization goal is to minimize $\frac{1}{2}\|Z - Y\|_2^2$, where Z is the output multi-channel signal defined in Equation (2). During training, we use an Adam optimizer with a learning rate of 0.1 and a weight decay of $5e-4$. We allow a maximum of 500 epochs, and stop iteration when the difference of losses between two epochs is less than $1e-4$.

For baselines, we choose the Monomial basis, Bernstein basis, Chebyshev basis (with Chebyshev interpolation) corresponding to GPRGNN, BernNet and ChebNetII, respectively. We also include arbitrary orthonormal basis learned by Favard for comparison. Note that, we learn *different filters on each channel for all baseline basis* for fairness.

Results. We exhibit the mean MSE losses with standard errors of the 60 samples achieved by different bases in Table 5. Optbasis, which promises the best convergence property, demonstrates an overwhelming advantage. A special note is needed that, the Monomial basis has *not finished converging* at the maximum allowed 500th epoch. In Section 5.4, we extend the maximum allowed epochs to 10,000, and use the slowly-converging Monomial basis curve as a counterpoint to the non-converging Favard curve.

Particularly, in Figure 2, we visualize the converging process on **one sample**. Obviously, OptBasis show **best convergence property** in terms of both the fastest speed and smallest MSE error. Check Appendix D.2 for more samples.

5.4. Non-Convergence of FavardGNN

Notably, in Figure 2, an obvious *bump* appeared near the 130th epoch. We now re-examine the non-convergence problem of FavardGNN (Section 3.3). We rerun the multichannel filter learning task by canceling early stopping and stretching the epoch number to 10,000. As shown in Figure 3 (left), the curve of Favard bump several times. In contrast with Favard is the Monomial basis, though showing

Table 5. Experimental results of the multichannel filtering learning task. *MSE loss \pm standard errors* of the 60 samples achieved by different bases are exhibited.

BASIS	OptBasis	ChebII	Bernstein	Favard	Monomial
MSE	0.0058	0.1501	0.4231	0.3175	3.9076
\pm STDV	\pm 0.0157	\pm 0.2433	\pm 0.4918	\pm 0.2840	\pm 2.9263

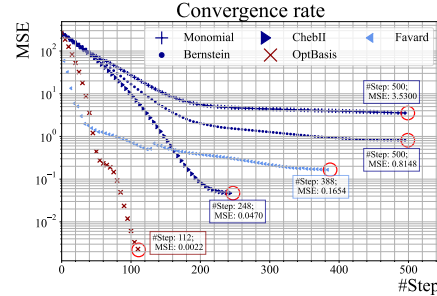


Figure 2. Convergence rate of minimizing $\frac{1}{2}\|Z - Y\|_2^2$ on one sample. *Sample message:* The true filters for this sample are low-pass(Y) / band-reject(Cb) / band-reject(Cr). *Legends:* ChebII means using Chebyshev polynomials combined with interpolation on chebynodes as in ChebNetII (He et al., 2022). Favard means the bases are learned as FavardGNN. In 500 epochs, the experimental groups of the Monomial basis and Bernstein basis did not converge. OptBasis achieves the smallest MSE error in the shortest time.

an inferior performance in Table 5, it converges slowly but stably. We observe a similar phenomenon with a node classification setup in Figure 3 (right) (See Appendix D.3 for details). Still, very large bumps appear. Such a phenomenon might seem contradictory to the outstanding performance of FavardGNN in node classification tasks. We owe the good performances in Table 1 and 2 to the early stop mechanism.

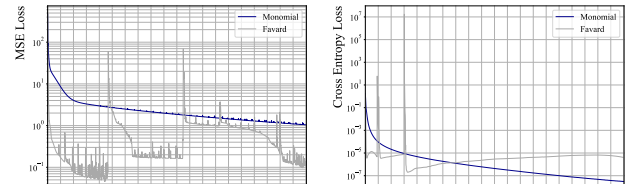


Figure 3. Drop of loss in 10,000 epochs. *Left:* MSE loss of regression task on one sample. *Right:* Cross entropy loss of classification problem on the Chameleon dataset. Models based on Monomial basis converge slowly, but stably. while FavardGNNs don't converge. For the convergence curve for OptBasis, please check Figure 2. It converges much faster than Monomial Basis.

6. Conclusion

In this paper, we tackle the fundamental challenges of basis learning and computation in polynomial filters. We propose two models: FavardGNN and OptBasisGNN. FavardGNN learns arbitrary basis from the whole space of orthonormal polynomials, which is rooted in classical theorems in orthonormal polynomials. OptBasisGNN leverages the optimal basis defined in Wang & Zhang (2022) efficiently, which was thought unsolvable. Extensive experiments are conducted to demonstrate the effectiveness of our proposed models. An interesting future direction is to derive a convex and easier-to-optimize algorithm for FavardGNN.

References

Abu-El-Haija, S., Perozzi, B., Kapoor, A., Alipourfard, N., Lerman, K., Harutyunyan, H., Steeg, G. V., and Galstyan, A. Mixhop: Higher-order graph convolutional architectures via sparsified neighborhood mixing. In Chaudhuri, K. and Salakhutdinov, R. (eds.), *Proceedings of the 36th International Conference on Machine Learning, ICML 2019, 9-15 June 2019, Long Beach, California, USA*, volume 97 of *Proceedings of Machine Learning Research*, pp. 21–29. PMLR, 2019. URL <http://proceedings.mlr.press/v97/abu-el-haija19a.html>.

Akiba, T., Sano, S., Yanase, T., Ohta, T., and Koyama, M. Optuna: A next-generation hyperparameter optimization framework. In Teredesai, A., Kumar, V., Li, Y., Rosales, R., Terzi, E., and Karypis, G. (eds.), *Proceedings of the 25th ACM SIGKDD International Conference on Knowledge Discovery & Data Mining, KDD 2019, Anchorage, AK, USA, August 4-8, 2019*, pp. 2623–2631. ACM, 2019. doi: 10.1145/3292500.3330701. URL <https://doi.org/10.1145/3292500.3330701>.

Balcilar, M., Renton, G., Héroux, P., Gaüzère, B., Adam, S., and Honeine, P. Analyzing the expressive power of graph neural networks in a spectral perspective. In *9th International Conference on Learning Representations, ICLR 2021, Virtual Event, Austria, May 3-7, 2021*. OpenReview.net, 2021. URL <https://openreview.net/forum?id=-qh0M9XWxnv>.

Chen, M., Wei, Z., Ding, B., Li, Y., Yuan, Y., Du, X., and Wen, J. Scalable graph neural networks via bidirectional propagation. *CoRR*, abs/2010.15421, 2020a. URL <https://arxiv.org/abs/2010.15421>.

Chen, M., Wei, Z., Huang, Z., Ding, B., and Li, Y. Simple and deep graph convolutional networks. In *Proceedings of the 37th International Conference on Machine Learning, ICML 2020, 13-18 July 2020, Virtual Event*, volume 119 of *Proceedings of Machine Learning Research*, pp. 1725–1735. PMLR, 2020b. URL <http://proceedings.mlr.press/v119/chen20v.html>.

Chien, E., Peng, J., Li, P., and Milenkovic, O. Adaptive universal generalized pagerank graph neural network. In *9th International Conference on Learning Representations, ICLR 2021, Virtual Event, Austria, May 3-7, 2021*. OpenReview.net, 2021. URL <https://openreview.net/forum?id=n6jl7fLxrP>.

Defferrard, M., Bresson, X., and Vandergheynst, P. Convolutional neural networks on graphs with fast localized spectral filtering. In Lee, D. D., Sugiyama, M., von Luxburg, U., Guyon, I., and Garnett, R. (eds.), *Advances in Neural Information Processing Systems 29: Annual Conference on Neural Information Processing Systems 2016, December 5-10, 2016, Barcelona, Spain*, pp. 3837–3845, 2016. URL <https://proceedings.neurips.cc/paper/2016/hash/04df4d434d481c5bb723be1b6df1ee65-Abstract.html>.

Favard, J. Sur les polynomes de tchebicheff. *CR Acad. Sci. Paris*, 200(2052-2055):11, 1935.

Gautschi, W. *Orthogonal polynomials: computation and approximation*. OUP Oxford, 2004.

Geronimo, J. and Van Assche, W. Approximating the weight function for orthogonal polynomials on several intervals. *Journal of Approximation Theory*, 65(3):341–371, 1991. ISSN 0021-9045. doi: [https://doi.org/10.1016/0021-9045\(91\)90096-S](https://doi.org/10.1016/0021-9045(91)90096-S). URL <https://www.sciencedirect.com/science/article/pii/002190459190096S>.

Hammond, D. K., Vandergheynst, P., and Gribonval, R. Wavelets on graphs via spectral graph theory. *CoRR*, abs/0912.3848, 2009. URL <http://arxiv.org/abs/0912.3848>.

He, M., Wei, Z., Huang, Z., and Xu, H. Bernnet: Learning arbitrary graph spectral filters via bernstein approximation. In Ranzato, M., Beygelzimer, A., Dauphin, Y. N., Liang, P., and Vaughan, J. W. (eds.), *Advances in Neural Information Processing Systems 34: Annual Conference on Neural Information Processing Systems 2021, NeurIPS 2021, December 6-14, 2021, virtual*, pp. 14239–14251, 2021. URL <https://proceedings.neurips.cc/paper/2021/hash/76f1cf7754a6e4fc3281bcccb3d0902-Abstract.html>.

He, M., Wei, Z., and Wen, J.-R. Convolutional neural networks on graphs with chebyshev approximation, revisited. *arXiv preprint arXiv:2202.03580*, 2022.

Hu, W., Fey, M., Zitnik, M., Dong, Y., Ren, H., Liu, B., Catasta, M., and Leskovec, J. Open graph benchmark: Datasets for machine learning on graphs. In Larochelle, H., Ranzato, M., Hadsell, R., Balcan, M., and Lin, H. (eds.), *Advances in Neural Information Processing Systems 33: Annual Conference on Neural Information Processing Systems 2020, NeurIPS 2020, December 6-12, 2020, virtual*, 2020. URL <https://proceedings.neurips.cc/paper/2020/hash/fb60d411a5c5b72b2e7d3527cfc84fd0-Abstract.html>.

Kingma, D. P. and Ba, J. Adam: A method for stochastic optimization. In Bengio, Y. and LeCun, Y. (eds.),

3rd International Conference on Learning Representations, ICLR 2015, San Diego, CA, USA, May 7-9, 2015, Conference Track Proceedings, 2015. URL <http://arxiv.org/abs/1412.6980>.

Kipf, T. N. and Welling, M. Semi-supervised classification with graph convolutional networks. In 5th International Conference on Learning Representations, ICLR 2017, Toulon, France, April 24-26, 2017, Conference Track Proceedings. OpenReview.net, 2017. URL <https://openreview.net/forum?id=SJU4ayYgl>.

Klicpera, J., Bojchevski, A., and Günnemann, S. Predict then propagate: Graph neural networks meet personalized pagerank. In 7th International Conference on Learning Representations, ICLR 2019, New Orleans, LA, USA, May 6-9, 2019. OpenReview.net, 2019. URL <https://openreview.net/forum?id=H1gL-2A9Ym>.

Lim, D., Hohne, F., Li, X., Huang, S. L., Gupta, V., Bhalerao, O., and Lim, S. Large scale learning on non-homophilous graphs: New benchmarks and strong simple methods. In Ranzato, M., Beygelzimer, A., Dauphin, Y. N., Liang, P., and Vaughan, J. W. (eds.), *Advances in Neural Information Processing Systems 34: Annual Conference on Neural Information Processing Systems 2021, NeurIPS 2021, December 6-14, 2021, virtual*, pp. 20887-20902, 2021. URL <https://proceedings.neurips.cc/paper/2021/hash/ae816a80e4c1c56caa2eb4e1819cbb2f-Abstract.html>.

Pei, H., Wei, B., Chang, K. C., Lei, Y., and Yang, B. Geom-gcn: Geometric graph convolutional networks. In 8th International Conference on Learning Representations, ICLR 2020, Addis Ababa, Ethiopia, April 26-30, 2020. OpenReview.net, 2020. URL <https://openreview.net/forum?id=S1e2agrFvS>.

Sen, P., Namata, G., Bilgic, M., Getoor, L., Galligher, B., and Eliassi-Rad, T. Collective classification in network data. *AI magazine*, 29(3):93–93, 2008.

Shaik, K. B., Ganesan, P., Kalist, V., Sathish, B., and Jenitha, J. M. M. Comparative study of skin color detection and segmentation in hsv and ycbcr color space. *Procedia Computer Science*, 57:41–48, 2015.

Shuman, D. I., Ricaud, B., and Vandergheynst, P. Vertex-frequency analysis on graphs. *CoRR*, abs/1307.5708, 2013. URL <http://arxiv.org/abs/1307.5708>.

Simon, B. Orthogonal polynomials on the unit circle, part 1: Classical theory, ams colloq, 2005.

Simon, B. Spectral theory of orthogonal polynomials. In *XVIIth International Congress on Mathematical Physics*, pp. 217–228. World Scientific, 2014.

Wang, G., Ying, R., Huang, J., and Leskovec, J. Improving graph attention networks with large margin-based constraints. *CoRR*, abs/1910.11945, 2019. URL <http://arxiv.org/abs/1910.11945>.

Wang, X. and Zhang, M. How powerful are spectral graph neural networks. In Chaudhuri, K., Jegelka, S., Song, L., Szepesvári, C., Niu, G., and Sabato, S. (eds.), *International Conference on Machine Learning, ICML 2022, 17-23 July 2022, Baltimore, Maryland, USA*, volume 162 of *Proceedings of Machine Learning Research*, pp. 23341–23362. PMLR, 2022. URL <https://proceedings.mlr.press/v162/wang22am.html>.

Wu, F., Zhang, T., Jr., A. H. S., Fifty, C., Yu, T., and Weinberger, K. Q. Simplifying graph convolutional networks. *CoRR*, abs/1902.07153, 2019. URL <http://arxiv.org/abs/1902.07153>.

Xu, K., Zhang, M., Jegelka, S., and Kawaguchi, K. Optimization of graph neural networks: Implicit acceleration by skip connections and more depth. volume 139, pp. 11592–11602, 2021.

Yang, Z., Cohen, W. W., and Salakhutdinov, R. Revisiting semi-supervised learning with graph embeddings. In Balcan, M. and Weinberger, K. Q. (eds.), *Proceedings of the 33rd International Conference on Machine Learning, ICML 2016, New York City, NY, USA, June 19-24, 2016*, volume 48 of *JMLR Workshop and Conference Proceedings*, pp. 40–48. JMLR.org, 2016. URL <http://proceedings.mlr.press/v48/yang16.html>.

A. Notations

Table 6. Summation of notations in this paper.

Notation	Description
$G = (V, E)$	Undirected, connected graph
N	Number of nodes in G
\hat{P}	Symmetric-normalized adjacency matrix of G .
\hat{L}	Normalized Laplacian matrix of G . $\hat{L} = I - \hat{P}$.
λ_i	The i -th eigenvalue of \hat{L} .
μ_i	The i -th eigenvalue of \hat{P} . $\mu_i = 1 - \lambda_i$.
U	Eigen vectors of \hat{L} and \hat{P} .
x	Input signal on 1 channel.
$X \in \mathbb{R}^{N \times d}$	Input features / Input signals on d channels.
$Z \in \mathbb{R}^{N \times d}$	Filtered signals.
$h(\cdot), b(\cdot)$	Filtering function defined on \hat{L} and \hat{P} , respectively. $h(\lambda) \equiv b(1 - \lambda)$.
$h_i(\cdot), b_i(\cdot)$	Filtering function on the i th signal channel. $X_{i,:} = h_i(\hat{L})Z_{i,:}$.
$h(\hat{L})x, b(\hat{P})x$	Filtering operation on signal x . $h(\hat{L}) \equiv b(\hat{P})$.
$\{g_k(\cdot)\}_{k=0}^K$	A polynomial basis of truncated order K .
$\{\alpha_k\}_{k=0}^K$	Coefficients above a basis. i.e. $h(\lambda) \approx \sum_{k=0}^K \alpha_k g_k(\lambda)$.

B. Proofs

This section is for the convenience of interested readers. We provided our proofs about the theorems (except for the original form of Favard's Theorem) and their relations used across our paper, although the theorems can be found in early chapters of monographs about orthogonal polynomials (Gautschi, 2004; Simon, 2014). We assume a relatively minimal prior background in orthogonal polynomials.

B.1. Three-term Recurrences for Orthogonal Polynomials (With Proof)

Theorem B.1 (Three-term Recurrences for Orthogonal Polynomials). (Simon, 2005, p. 12) *For any orthogonal polynomial series $\{p_k(x)\}_{k=0}^{\infty}$, suppose that the leading coefficients of all polynomial are positive, the series satisfies the recurrence relation:*

$$p_{k+1}(x) = (A_k x + B_k)p_k(x) + C_k p_{k-1}(x), \\ p_{-1}(x) := 0, A_k, C_k \in \mathbb{R}^+, B_k \in \mathbb{R}, k \geq 0.$$

Proof. The core part of this proof is that xp_k is orthogonal to p_i for $i \leq k - 2$, i.e.

$$\langle xp_k, p_i \rangle = 0, \quad i \leq k - 2.$$

Since $xp_k(x)$ is of order $k + 1$, we can rewrite $xp_k(x)$ into the combination of first $k + 1$ polynomials of the basis:

$$xp_k(x) = \alpha_{k,k+1}p_{k+1}(x) + \alpha_{k,k}p_k(x) + \alpha_{k,k-1}p_{k-1}(x) + \cdots + \alpha_{k,0}p_0(x) \quad (7)$$

or in short,

$$xp_k(x) = \sum_{j=k+1}^0 \alpha_{k,j}p_j(x).$$

Project each term onto $p_i(x)$,

$$\langle xp_k(x), p_i(x) \rangle = \sum_{j=k+1}^0 \alpha_{k,j} \langle p_j(x), p_i(x) \rangle.$$

Using the orthogonality among $\{p_k(x)\}_{k=0}^{\infty}$, we have

$$\langle xp_k(x), p_i(x) \rangle = \langle \alpha_{k,i} p_i(x), p_i(x) \rangle \Rightarrow \alpha_{k,i} = \frac{\langle xp_k(x), p_i(x) \rangle}{\langle p_i(x), p_i(x) \rangle}. \quad (8)$$

Next, we show $\langle xp_k(x), p_i(x) \rangle = 0$ when $i \leq k - 2$. Since $\langle xp_k(x), p_i(x) \rangle \equiv \langle p_k(x), xp_i(x) \rangle$, it is equivalent to show $\langle p_k(x), xp_i(x) \rangle = 0$.

When $i \leq k - 2$, applying $xp_i(x) = \sum_{j=0}^{i+1} \alpha_{i,j} p_j(x)$ and the orthogonality between $p_j(x)$ and $p_k(x)$ when $j \neq k$, we get

$$\langle p_k, xp_i(x) \rangle = \sum_{j=0}^{i+1} \alpha_{i,j} \langle p_k, p_j(x) \rangle \stackrel{j \leq k-1}{=} 0 \Rightarrow \langle xp_k, p_i(x) \rangle = 0.$$

Therefore, $xp_k(x)$ is only relevant to $p_{k+1}(x)$, $p_k(x)$ and $p_{k-1}(x)$. By shifting items, we soonly get that: $p_{k+1}(x)$ is only relevant to $xp_k(x)$, $p_k(x)$ and $p_{k-1}(x)$.

At last, we show that, by regularizing the leading coefficients A_k to be positive, $C_k > 0$. Firstly, since the leading coefficients are positive, $\{\alpha_k\}_{k=0}^{\infty}$ defined in Equation (7) are positive. Then, notice from Equation (8), we get

$$-\frac{C_k}{A_k} = \alpha_{k,k-1} = \frac{\langle xp_k(x), p_{k-1}(x) \rangle}{\langle p_{k-1}(x), p_{k-1}(x) \rangle} = \frac{\langle p_k(x), xp_{k-1}(x) \rangle}{\langle p_{k-1}(x), p_{k-1}(x) \rangle} = \frac{\alpha_{k-1,k}}{\langle p_{k-1}(x), p_{k-1}(x) \rangle}.$$

We have finished our proof. \square

B.2. Favard's Theorem (Monomial Case)

Theorem B.2 (Favard's Theorem). (Favard, 1935) If a sequence of monic polynomials $\{P_n\}_{n=0}^{\infty}$ satisfies a three-term recurrence relation

$$P_{n+1}(x) = (x - \gamma_n) P_n(x) - \beta_n P_{n-1}(x),$$

with $\gamma_n, \beta_n \in \mathbb{R}, \beta_n > 0$, then $\{P_n\}_{n=0}^{\infty}$ is orthogonal with respect to some positive weight function.

B.3. Favard's Theorem (General Case) (With Proof)

Corollary B.3 (Favard's Theorem; general case). If a sequence of polynomials $\{P_n\}_{n=0}^{\infty}$ statisfies a three-term recurrence relation

$$P_{n+1}(x) = (\varsigma_n x - \gamma_n) P_n(x) - \beta_n P_{n-1}(x),$$

with $\gamma_n, \beta_n, \varsigma_n \in \mathbb{R}, \varsigma_n \neq 0, \beta_n/\varsigma_n > 0$, then there exists a positive weight function w such that $\{P_n\}_{n=0}^{\infty}$ is orthogonal with respect to the inner product $\langle p, q \rangle = \int_{\mathbb{R}} p(x)q(x)w(x)dx$.

Proof. Set $\gamma_n^* = \frac{\alpha_n}{\varsigma_n}, \beta_n^* = \frac{\beta_n}{\varsigma_n}$. Then we can construct a sequence of polynomials $\{P_n^*\}_{n=0}^{\infty}$.

Case 1: For $n = 0$ and $n = 1$, set $P_n^* := P_n(x)/\hat{P}_n(x)$.

Case 2: For $n \geq 2$, define $P_n^*(x)$ by the three-term recurrences:

$$P_{n+1}^*(x) := (x - \gamma_n^*) P_n^*(x) - \beta_n^* P_{n-1}^*(x).$$

According to Theorem B.2, $\{P_n^*\}_n$ is an orthogonal basis. Since P_n is scaled P_n^* by some constant, so $\{P_n\}_n$ is also orthogonal. \square

B.4. Proof of Theorem 3.1

We restate the Theorem of three-term recurrences for orthonormal polynomials (Theorem 3.1) as below, and give a proof.

(Three Term Recurrences for Orthonormal Polynomials) For orthonormal polynomials $\{p_k\}_{k=0}^{\infty}$ w.r.t. weight function w , suppose that the leading coefficients of all polynomial are positive, there exists the three-term recurrence relation:

$$\begin{aligned}\sqrt{\beta_{k+1}}p_{k+1}(x) &= (x - \gamma_k)p_k(x) - \sqrt{\beta_k}p_{k-1}(x), \\ p_{-1}(x) &:= 0, \quad p_0(x) = 1/\sqrt{\beta_0}, \quad \gamma_k \in \mathbb{R}, \quad \sqrt{\beta_k} \in \mathbb{R}^+, \quad k \geq 0\end{aligned}$$

with $\beta_0 = \int w(x)dx$.

Proof. **Case 1:** $k = 0$. $p_k(x)$ is a constant. Suppose it to be t , then

$$\langle p_0(x), p_0(x) \rangle = t^2 \int_a^b d\alpha \Rightarrow t = 1/\sqrt{\beta_0}.$$

Case 2: $k \geq 1$. By Theorem B.1, since $\{p_k\}_{k=0}^K$ is orthogonal, there exist three term recurrences as such:

$$p_{k+1}(x) = (A_k x + B_k)p_k(x) + C_k p_{k-1}(x), \quad k = 1, 2, 3, \dots$$

By setting $c_k^* = \frac{1}{A_k}$, $a_k^* = -\frac{B_k}{A_k}$, $b_k^* = -\frac{C_k}{A_k}$, it can be rewritten into

$$c_k^* p_{k+1}(x) = (x - a_k^*)p_k(x) - b_k^* p_{k-1}(x), \quad k = 1, 2, 3, \dots \quad (9)$$

Apply dot products with $p_{k-1}(x)$ to Equation (9), we get

$$\begin{aligned}\langle x p_k(x), p_{k-1}(x) \rangle &= \langle b_k^* p_{k-1}(x), p_{k-1}(x) \rangle \\ \Rightarrow b_k^* &= \langle x p_k(x), p_{k-1}(x) \rangle \\ (k &= 1, 2, 3, \dots).\end{aligned} \quad (10)$$

Similarly, apply dot products with $p_{k+1}(x)$, we get:

$$\begin{aligned}\langle c_k^* p_{k+1}(x), p_{k+1}(x) \rangle &= \langle x p_k(x), p_{k+1}(x) \rangle \\ \Rightarrow c_k^* &= \langle x p_k(x), p_{k+1}(x) \rangle \\ \Rightarrow c_k^* &= \langle x p_{k+1}(x), p_k(x) \rangle \\ (k &= 1, 2, 3, \dots).\end{aligned} \quad (11)$$

Notice that in Equation (11)

$$\langle x p_k(x), p_{k+1}(x) \rangle = \langle p_k(x), x p_{k+1}(x) \rangle \stackrel{(10)}{=} b_{k+1}^*.$$

We get:

$$c_k^* = b_{k+1}^*.$$

So we can write Equation (9) into the form below:

$$b_{k+1}^* p_{k+1}(x) = (x - a_k^*)p_k(x) - b_k^* p_{k-1}(x), \quad k = 1, 2, 3, \dots$$

At last, we show $b_k^* > 0$.

Firstly, recall that $b_k^* = \langle x p_k(x), p_{k-1}(x) \rangle = \langle p_k(x), x p_{k-1}(x) \rangle$. Since $x p_{k-1}(x)$, which is of order k , can be written into the combination of $\{p_j\}_{j=0}^k$ which the leading coefficients to be non-zero, i.e.

$$x p_{k-1}(x) = a_{k,k} p_k(x) + a_{k,k-1} p_{k-1}(x) + \dots + a_{k,0} p_0(x) \quad (a_{k,k} \neq 0)$$

Secondly, since $\langle g(x), g(x) \rangle \equiv \langle -g(x), -g(x) \rangle$, we can restrict all the leading coefficients to be positive.

$$b_n^* = \langle p_k(x), x p_{k-1}(x) \rangle = a_{k,k} > 0.$$

Thus we have proved $b_k^* > 0$ holds.

Furthermore, we can rewrite b_k^* into $\sqrt{\beta_k}$. The proof is finished. \square

B.5. Proof of Theorem 3.2

We restate the Favard's Theorem for orthonormal polynomials (Theorem 3.2) as below, and give a proof based on the general case B.3.

(Favard Theorem; Orthonormal case) A polynomial series $\{p_k\}_{k=0}^{\infty}$ who satisfies the recurrence relation

$$\begin{aligned}\sqrt{\beta_{k+1}}p_{k+1}(x) &= (x - \gamma_k)p_k(x) - \sqrt{\beta_k}p_{k-1}(x), \\ p_{-1}(x) &:= 0, \quad p_0(x) = 1/\sqrt{\beta_0}, \quad \gamma_k \in \mathbb{R}, \quad \sqrt{\beta_k} \in \mathbb{R}^+, \quad k \geq 0\end{aligned}$$

is orthonormal w.r.t. a weight function w that $\beta_0 = \int w(x)dx$.

Proof. First of all, according to Theorem 3.2, the series $\{p_k\}_{k=0}^{\infty}$ is orthogonal.

Apply dot products with $p_{k-1}(x)$, we get

$$\begin{aligned}\langle xp_k(x), p_{k-1}(x) \rangle &= \left\langle \sqrt{\beta_k}p_{k-1}(x), p_{k-1}(x) \right\rangle \\ \Rightarrow \langle xp_k(x), p_{k-1}(x) \rangle &= \sqrt{\beta_k} \langle p_{k-1}(x), p_{k-1}(x) \rangle \\ &\quad (k = 0, 1, \dots).\end{aligned}$$

Similarly, apply dot products with $p_{k+1}(x)$, we get:

$$\begin{aligned}\left\langle \sqrt{\beta_{k+1}}p_{k+1}(x), p_{k+1}(x) \right\rangle &= \langle xp_k(x), p_{k+1}(x) \rangle \\ \Rightarrow \sqrt{\beta_{k+1}} \langle p_{k+1}(x), p_{k+1}(x) \rangle &= \langle xp_k(x), p_{k+1}(x) \rangle \\ &\quad (k = 0, 1, \dots),\end{aligned}$$

which can be rewritten as:

$$\begin{aligned}\sqrt{\beta_k} \langle p_k(x), p_k(x) \rangle &= \langle xp_{k-1}(x), p_k(x) \rangle \\ &\quad (k = 1, 2, \dots),\end{aligned}$$

Notice that

$$\langle xp_{k-1}(x), p_k(x) \rangle = \langle xp_k(x), p_{k-1}(x) \rangle.$$

We get:

$$\begin{aligned}\sqrt{\beta_k} \langle p_k(x), p_k(x) \rangle &= \langle xp_{k-1}(x), p_k(x) \rangle \\ &= \sqrt{\beta_k} \langle p_{k-1}(x), p_{k-1}(x) \rangle \\ \Rightarrow \langle p_k(x), p_k(x) \rangle &= \langle p_{k-1}(x), p_{k-1}(x) \rangle \\ &\quad (k = 1, 2, \dots),\end{aligned}$$

which indicates that the polynomials $\{p_k\}_{k=0}^K$ are same in their norm.

Since $p_0(x) \equiv 1/\sqrt{\beta_0}$ and $\beta_0 = \int w(x)dx$, $\langle p_0(x), p_0(x) \rangle = \frac{1}{\beta_0} \int w(x)dx = 1$. Thus the norm of every polynomial in $\{p_k\}_{k=0}^{\infty}$ equals 1.

Combining that $\{p_k\}_{k=0}^{\infty}$ is orthogonal and $\langle p_k(x), p_k(x) \rangle = 1$ for all k , we arrive that $\{p_k\}_{k=0}^{\infty}$ is an orthonormal basis. \square

B.6. Proof of Equation (6)

Proof. First, notice that

$$\langle v_{k+1}^*, v_{k-1} \rangle = \langle \hat{P}v_k, v_{k-1} \rangle = \langle v_k, \hat{P}v_{k-1} \rangle.$$

On the other hand,

$$\|v_{k+1}^{\perp}\| = \langle v_{k+1}, v_{k+1}^{\perp} \rangle = \langle v_{k+1}, v_{k+1}^* \rangle = \langle v_{k+1}, \hat{P}v_k \rangle.$$

So, we get

$$\|v_k^{\perp}\| = \langle v_k, \hat{P}v_{k-1} \rangle = \langle \hat{P}v_k, v_{k-1} \rangle = \langle v_{k+1}^*, v_{k-1} \rangle.$$

\square

Thus, we have finished our proof.

C. Pseudo-codes

C.1. Pseudo-code for FavardGNN.

Algorithm 7: FavardGNN.Pytorch style.

```
# f: raw feature dimension
# d: hidden dimension, or number of channels
# N: number of nodes
# K: order of polynomial basis
# X(Nxd): Input features
# P(NxN): Sym-normalized adjacency matrix
# Coef(dx(K+1)): coefficient matrix
# SqrtBeta(dx(K+1)): Coefficients for three-term recurrences
# Gamma(dx(K+1)): Coefficients for three-term recurrences

# Transfer raw input in signals
X = ReLU(MLP(X.dropout())).dropout() # (Nxd)

SqrtBeta = torch.clamp(norm, 1e-2)

# Process H_0
H_0 = X / SqrtBeta[:,0] # (Nxd)

Z = torch.zeros_like(X)
# Add to the final representation
Z = Z + torch.einsum('Nd,d->Nd', H_0, Coef[:,0])

last_H = H_0
second_last_H = torch.zeros_like(H_0)

for k in range(1, K):
    # Three-term Recurrence Formula for Orthonormal Polynomials
    H_k = P @ last_H # (Nxd)
    H_k = H_k - Gamma[k,:].unsqueeze(0)*last_H - SqrtBeta[k,:].unsqueeze(0)*second_last_H
    H_k = H_k / SqrtBeta[k+1,:].unsqueeze(0)

    # Add to the final representation
    Z = Z + torch.einsum('Nd,d->Nd', H_k, Coef[:,k])

# Transform the final representation into predictions
Y = MLP(ReLU(Z).dropout())
Pred = Softmax(Y)
return Pred
```

C.2. Pseudo-code for OptBasisGNN.

Algorithm 8: OptBasisGNN. Pytorch style.

```

# f: raw feature dimension
# d: hidden dimension, or number of channels
# N: number of nodes
# K: order of polynomial basis
# X(Nxd): Input features
# P(NxN): Sym-normalized adjacency matrix
# Coef(dxK): coefficient matrix

# Transfer raw input in signals
X = ReLU(MLP(X.dropout())).dropout() # (Nxd)

# Normalize H_0
norm = torch.norm(X, dim=0).view(1, d)
norm = torch.clamp(norm, 1e-8)
H_0 = X / norm # (Nxd)

Z = torch.zeros_like(X)
# Add to the final representation
Z = Z + torch.einsum('Nd,d->Nd', H_0, Coef[:,0])

last_H = H_0
second_last_H = torch.zeros_like(H_0)

for k in range(1, K):
    H_k = P @ last_H # (Nxd)

    # Orthogonalize H_k to all the former vectors
    # To achieve this, only 2 subtractions are required
    project_1 = torch.einsum('Nd,Nd->1d', H_k, last_H) # (1xd)
    project_2 = torch.einsum('Nd,Nd->1d', H_k, second_last_H) # (1xd)
    H_k = H_k - project_1 * last_H - project_2 * second_last_H # (Nxd)

    # Normalize H_k
    norm = torch.norm(H_k, dim=0).view(1, d)
    norm = torch.clamp(norm, 1e-8)
    H_k = H_k / norm # (Nxd)

    # Add to the final representation
    Z = Z + torch.einsum('Nd,d->Nd', H_k, Coef[:,k])

# Transform the final representation to predictions
Y = MLP(ReLU(Z).dropout())
Pred = Softmax(Y)
return Pred

```

D. Experimental Settings.

D.1. Node Classification Tasks on Large and Small Datasets.

Model setup. The structure of FavardGNN and OptBasisGNN follow Algorithm 2. The hidden size of the first MLP layers h is set to be 64, which is also the number of filter channels. For the scaled-up OptBasisGNN, we drop the first MLP layer to fix the basis vectors needed for precomputing, and following the scaled-up version of ChebNetII (He et al., 2022), we add a three-layer MLP with weight matrices of shape $F \times h$, $h \times h$ and $h \times c$ after the filtering process.

For both models, the initialization of α is set as follows: for each channel l , the coefficients of the $g_{0,l}$ are set to be 1, while the other coefficients are set as zeros, which corresponds to initializing the polynomial filter on each channel to be $h(\lambda) = 1 - \lambda$. For the initialization of three-term parameters that determine the initial polynomial bases on each channel, we simply set $\{\sqrt{\beta}\}$ to be ones, and $\{\gamma\}$ to be zeros.

Hyperparameter tunning. For the optimization process on the training sets, we tune all the parameters with Adam (Kingma & Ba, 2015) optimizer. We use early stopping with a patience of 300 epochs.

We choose hyperparameters on the validation sets. To accelerate hyperparameter choosing, we use Optuna(Akiba et al., 2019) to select hyperparameters from the range below with a maximum of 100 complete trials³:

1. Truncated Order polynomial series: $K \in \{2, 4, 8, 12, 16, 20\}$;

³We use Optuna's Pruner to drop some hyperparameter choice in an early stay of training. This is called an incomplete/pruned trial.

2. Learning rates: $\{0.0005, 0.001, 0.005, 0.1, 0.2, 0.3, 0.4, 0.5\}$;
3. Weight decays: $\{1e-8, \dots, 1e-3\}$;
4. Dropout rates: $\{0., 0.1, \dots, 0.9\}$;

There are two extra hyperparameters for scaled-up OptBasisGNN:

1. Batch size: $\{10,000, 50,000\}$;
2. Hidden size (for the post-filtering MLP): $\{512, 1024, 2048\}$.

D.2. Multi-Channel Filter Learning Task.

YCbCr Channels. We put the practical background of our multichannel experiment in the YCbCr color space, a useful color space in computer vision and multi-media (Shaik et al., 2015).

Our Synthetic Dataset. When creating our datasets with 60 samples, we use 4 filter combinations on 15 images in He et al. (2021)'s single filter learning datasets. The 4 combinations on the three channels are:

1. Band-reject(Y) / low-pass(Cb) / high-pass(Cr);
2. High-pass(Y) / High-pass(Cb) / low-pass(Cr);
3. High-pass(Y) / low-pass(Cb) / High-pass(Cr);
4. Low-pass(Y) / band-reject(Cb) / band-reject(Cr).

The concrete definitions of the signals, i.e. band-reject are aligned with those given in He et al. (2022).

Visualization on more samples. We visualize more samples as Figure 2 in Figure 4. In all the samples, the tendencies of different curves are alike.

D.3. Examining of FavardGNN's bump.

Figure 3 (right), we observe bump with a node classification setup. To show this clearer, we let FavardGNN and GPRGNN (which uses the Monomial basis for classification) to fit *the whole set* of nodes, and move dropout and Relu layers. As in the regression re-examine task, we cancel the earlystop mechanism, stretch the epoch number to 10,000, and record cross entropy loss on each epoch.

E. Summary of Wang's work

This section is a restate for a part of Wang & Zhang (2022). For the convenience of the reader's reference, we write this section here. More interested readers are encouraged to refer to the original paper.

Wang & Zhang (2022) raise a criterion for best basis, but states that it **cannot be reached**.

E.1. The Criterion for Optimal Basis

Following Xu et al. (2021), Wang & Zhang (2022) considers the squared loss $R = \frac{1}{2}\|Z - Y\|_F^2$, where Y is the target, and $Z = \left\| \sum_{l=1}^L \sum_{k=0}^K \alpha_{k,l} g_{k,l}(\hat{P}) X_{:,l} \right\|_F^2$.⁴

Since each signal channel is independent and contributes independently to the loss, i.e. $R = \sum_l \frac{1}{2}\|Z_{:,l} - Y_{:,l}\|_F^2$, we can then consider the loss function channelwisely and ignore l . Loss on one signal channel x is:

$$r = \frac{1}{2}\|z - y\|_F^2,$$

where $z = \sum_{k=0}^K \alpha_k g_k(\hat{P}) x$.

This loss is a convex function w.r.t. α . Therefore, the gradient descents's convergence rate depends on the **Hessian matrix**'s condition number, denoted as $\kappa(H)$. When H is an identity matrix, $\kappa(H)$ reaches minimum and leads to best convergence

⁴Here, X is not necessarily the raw feature (X_{raw}) but often some thing like $X_{raw}W$. W is irrelavant to the choice of polynomial basis, and merges W into X .

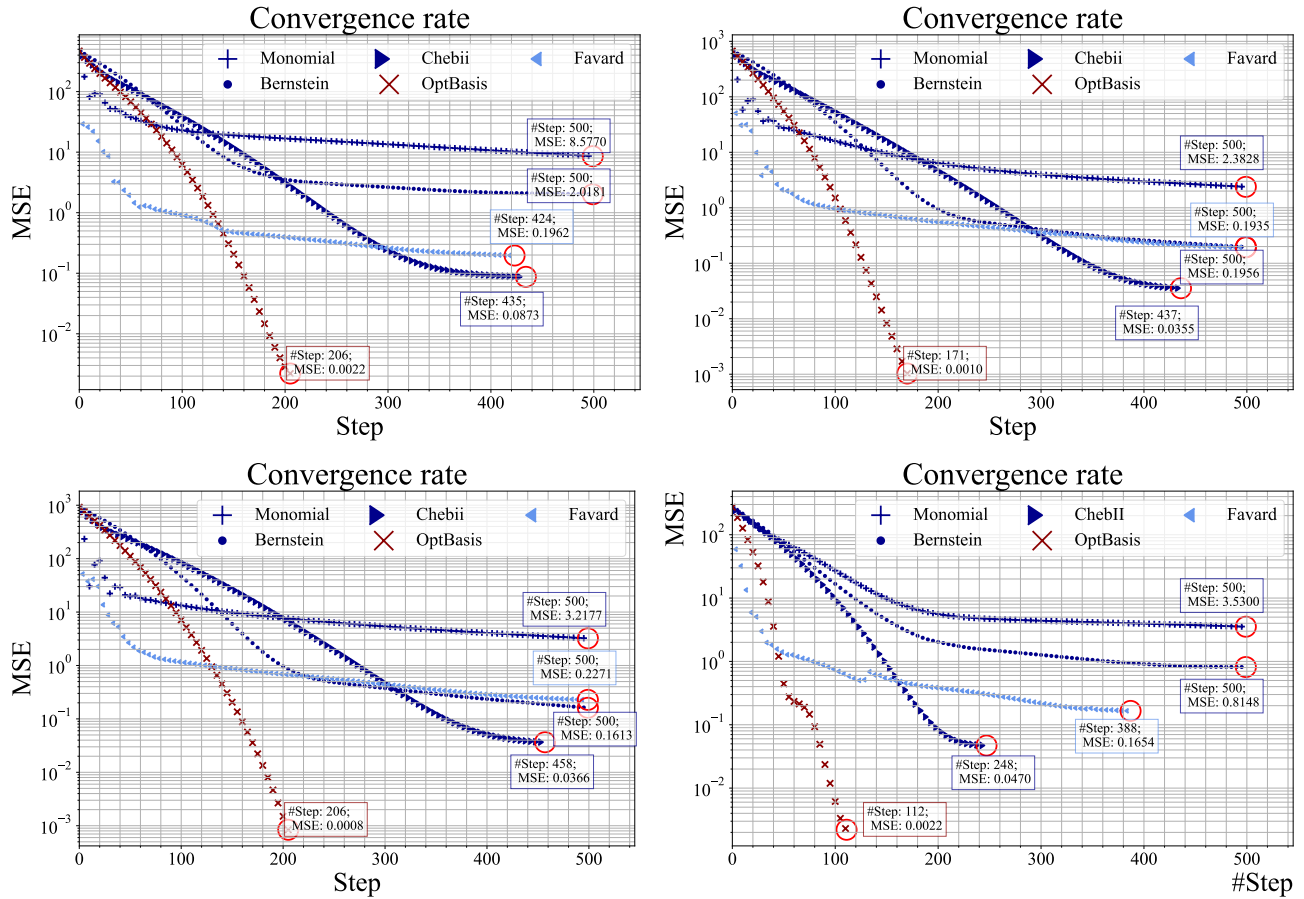


Figure 4. Visualization with more samples in the multi-channel filter learning task.

rate (Boyd & Vandenberghe, 2009).

The Hessian matrix H looks like⁵:

$$H_{k_1 k_2} = \frac{\partial r}{\partial \alpha_{k_1} \alpha_{k_2}} = x^T g_{k_2}(\hat{P}) g_{k_1}(\hat{P}) x.$$

Wang & Zhang (2022) further write $H_{k_1 k_2}$ in the following form:

$$H_{k_1 k_2} = x^T g_{k_2}(\hat{P}) g_{k_1}(\hat{P}) x = \sum_{i=1}^n g_{k_1}(\mu_i) g_{k_2}(\mu_i) (U^T x)_i^2,$$

which can be equivalently expressed as a Riemann sum:

$$\sum_{i=1}^N g_{k_1}(\mu_i) g_{k_2}(\mu_i) \frac{F(\mu_i) - F(\mu_{i-1})}{\mu_i - \mu_{i-1}} (\mu_i - \mu_{i-1}),$$

where $F(\mu) := \sum_{\mu_i \leq \mu} (U^T x)_i^2$. Define $f(\mu) = \frac{\Delta F(\mu)}{\Delta \mu}$, $H_{k_1 k_2}$ comes to

$$H_{k_1 k_2} = \int_{\mu=-1}^1 g_{k_1}(\mu) g_{k_2}(\mu) f(\mu) d\mu.$$

This suggests that, $\{g_k\}_{k=1}^N$ is an optimal basis when it is **orthonormal** w.r.t. **weight function** $f(\cdot)$. (For more about orthonormal basis, see Section 2.2.)

E.2. Wang's Method

Having write out the weight function $f(\mu)$, the optimal basis is determined. Wang & Zhang (2022) think of a regular process for getting this optimal basis, which is unreachable since eigen-decomposition is unaffordable for large graphs. We summarize this process in Algorithm 3.

According to Wang & Zhang (2022), the optimal basis would be an orthonormal basis, but unfortunately, this basis and the exact form of its weight function is unattainable. As a result, they come up with a compromise by allowing the model to choose from the orthogonal Jacobi bases, which have “*flexible enough weight functions*”, i.e. $(1-\mu)^\alpha (1+\mu)^\beta$. The Jacobi bases are a family of polynomial bases. A specific form Jacobi basis is determined by two parameters (α, β) . Similar to the well-known Chebyshev basis, Jacobi bases have a recursive formulation, making them efficient for calculation.

⁵Note that, Wang & Zhang (2022) define g_{k_2} on \hat{L} (or $\{\lambda_i\}$) while we define it on \hat{P} (or $\{\mu_i\}$). They are equivalent.